ICAS 2016
30th Congress of the International Council of the Aeronautical Sciences
DCC, Daejeon, Korea ; September 25-30, 2016

EXPERIMENTAL ANALYSES OF DROOP, WINGTIPS AND FENCES ON A BWB MODEL

H. D. Cerón-Muñoz*, D. O. Diaz-Izquierdo*, P. D. Bravo-Mosquera *, F. M. Catalano *, L. D. de Santana.**
***São Carlos Engineering School-University of São Paulo-Brazil.**
****University of Twente - Netherlands**
Keywords: *Blended Wing Body, C-Wing, Winglet.*

Abstract

This work performs wind-tunnel tests to analyze the aerodynamics of wingtip devices and fences in a blended wing body aircraft (BWB). The Green aircraft concept has the BWB as a promising solution which optimally combines low-noise, fuel efficiency and consequently low-emission. This innovative approach has been consistently investigated by the Aircraft Laboratory of the São Carlos Engineering School – University of São Paulo. In previous developments, this laboratory showed the presence of cross flow on the external part of the body and an stronger vortex in the middle of the model. To avoid this undesirable effect, the first prototype has been improved by the addition of a droop and three fences. Additionally winglets and C-wings were considered in this research. Results show that wingtip devices improved the aerodynamic efficiency by the generation of an aerodynamic resultant force which has a component in the direction of the flight reducing the total drag. On the other hand, the fences showed improved efficiency at higher angles of attack.

1 Introduction

The Blended Wing Body concept (**BWB**) has been presented about three decades ago as an environmental friendly alternative able to carry the largest payload through the greatest distance with the lowest fuel consumption. From the aerodynamic standing point, the BWB concept is simple since it integrates in one single body a smooth combination of wings, fuselage, tail and propulsion system [1, 2]. This allows to reduce the airplane wet area and the aerodynamic interference present the junction of the lifting parts. The BWB satisfies current and future environmental restrictions regarding fuel emissions and noise and brings low direct operating cost (DOC) per passenger [3].

The common sense regarding the aerodynamic advantages of the BWB configuration are offset by open questions to be resolved: The cabin pressurization system brings new challenges due to the non-cylindrical fuselage geometry; The reduced number of passengers with direct access to the windows brings discomfort and difficulties to the emergency evacuation; This new configuration requires a totally new control system architecture; furthermore new set of materials required in this design imposes high risks to the certification.

Current commercial aircraft designs follows predominantly the so-called “conventional configuration”. In this geometry the tubular fuselage is joint to swept, tapered and high aspect ratio wings, which by turn hangs the engine, and the stabilizer surfaces are normally placed in the back of the airplane [4]. This shape reached the state-of-the-art, therefore one can notice that the graphs which show, the yearly improvement of productivity and performance have reached an asymptotic behavior, consequently, only a break of paradigm can bring further progress to the aviation [5].

In the BWB configuration, the payload is allocated inside the spacious structure in a winged shape. The aircraft weight is reduced by eliminating the stabilizers resulting into drag reduction and improved maneuverability. In the

firsts BWBs, the aerodynamic advantages were cancelled by the longitudinal and lateral stability constraints, however, the combination of swept wings, elevators and ailerons, corrected this problems[7]. In 1989 the first BWB generation has been presented as alternative to the future of aircraft transport[8]. In 2006, the silent aircraft project, called SAX("**S**ilence **A**ircraft e**X**perimental"), was launched[9]. The Silent Aircraft initiative was a multidisciplinary project that aims to reduce the noise emission to be imperceptible in the urban surroundings of the airports [3].

The São Paulo University's São Carlos Engineering School Aircraft Laboratory developed wind-tunnel testing in a BWB prototype. The main phenomena observed in those experiments are: stall at high angle-of-attack (α), with gradual stall process typical delta wings; at α=8°, the slope of the C_L vs. α curve decreases abruptly the drag growth rate became considerably high when compared to results obtained at low angles-of-attack. Oil flow visualization showed the presence of spanwise cross flow over the outer wing starting from the root going towards to the tip at $\alpha \geq 8^o$. This results could explain the slope decrease. Oppositely, at $\alpha \geq 12^o$ two large vortices are observed in the end of the model's central body. Figure 1 shows the BWB isometric view and oil flow visualization pictures. Detailed information is present at Cerón-Muñoz H. D et al. [6].

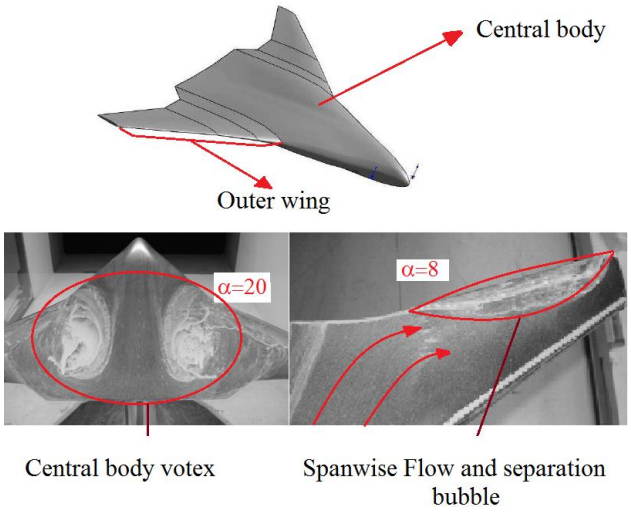

Fig 1. First prototype tested

This paper present the next stage of this research. To improve the outer wing aerodynamic behavior two alternatives are analyzed: firstly, aiming to delay the outer wing separation, a droop is added along the leading edge. secondly, wing fences are added to the wing such to avoid cross flow formation. Additionally, a C-wing and winglet are placed.

2 The wind-tunnel prototype

The BBW model is composed of a central body section and two tapered and swept wings smoothly linked, according to the proportions suggested by Qin et al.[10]. The swept-back angle is 56° on the central body and 38° at the outer wing at leading edge in the both cases.

The aspect ratio is AR=6,68 and the wetted area ratio is S_w/A_{ref} =3,06. The reference area and mean chord, used to the aerodynamic coefficients, are A_{ref} = 0,23 m^2 and C_{ref} = 0,20 m, respectively. The aircraft central body consists of five airfoils from the plane of symmetry of the aircraft, toward spanwise direction, located at: y/b = 0 ; 0,32; 0,64; 0,125 and 0,17. The model is constructed in fiberglass reinforced by carbon fiber laminated with the hand lay-up.

Two relevant factors are considered in the airfoils selection: thickness and low Reynolds number performance. Following this criteria Eppler airfoils were selected according to thickness distribution proposed by Quin et al. [10]. Additionally, the central body airfoils were modified to result into reflexed cambers and therefore lead to improved stability condition. Figure 2 shows the model placed in the wind-tunnel test section and the main geometric references. The BWB model studied in this paper is detailed in Cerón-Muñoz H. D et al. [6, 11].

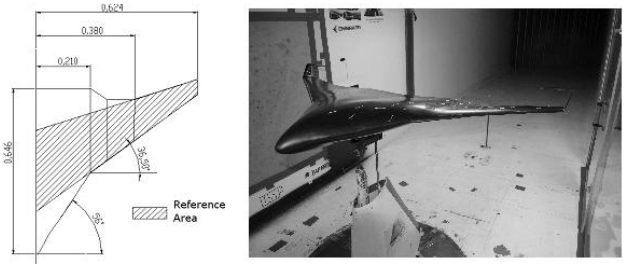

Fig 2. BWB model in the wind-tunnel

3 Experimental setup

The experimental campaign has been conducted in the São Paulo University's Aircraft Laboratory of the São Carlos Engineering School, Brazil. The closed section closed circuit wind-tunnel a presents a test section of 1.3 x 1.75 m^2, a turbulence level of 0.25 per cent and maximum speed of 40 m/s [12]. Following, each device analyzed is briefly described.

- **Droop**: This device, presented in Fig. 3, increases the camber in the leading edge region, consequently, the stall will be softer and the boundary layer separation will be delayed by some degrees.

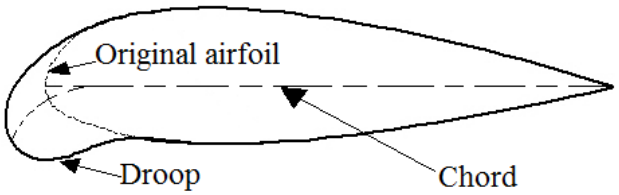

Fig 3 Leading edge droop

- **Wing-fences**: Wing fences are thin flat plates installed perpendicularly to the wing upper surface and distributed along the wing span. The wing-fences were developed by K. eWohlfart [13] and their goal is delaying the separation on swept wings at high angles of attack. Their height can be around 6% of the chord, following the order of magnitude of the thickness of the wing. Some types of WF are shown in Fig 4.

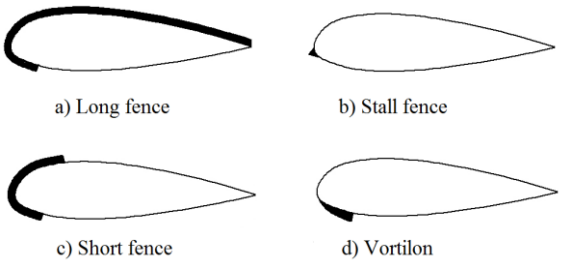

Fig 4. Wing-fence types

- **Winglets and C-Wings**: The Winglets are small wings located on the aircraft wingtip. These devices generate an aerodynamic force in the direction of flight reducing the drag. The winglet height is 6.3 cm, incidence angle at the winglet root 2^o, washout of 1^o. The cant and sweep angles were of 72^o and 32^o , respectively, and the relation tip/root chord was 0.55 accordingly to Whitcom[14]. For the C-Wing, an horizontal airfoil NACA 0012 was added to the winglet above, which has twist of 2^o (washout) and a semi-span of 11 cm. Figure 4 shows the two studied devices as and the aerodynamic forces.

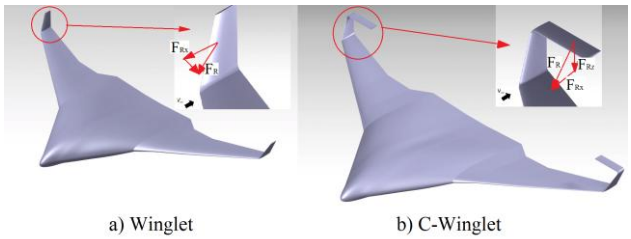

Fig 4 Wingtip devices

3.1 Tested configurations

The boundary layer transition is forced by a roughness strip built with sand adhered to the surface. On the outer wing, the transition region is located at 5% of the local chord on the upper surface. In the central body, the strip roughness followed the previous proportion, however, in the region equivalent to the nose, the transition was fixed transversely as can be seen in Fig 5.

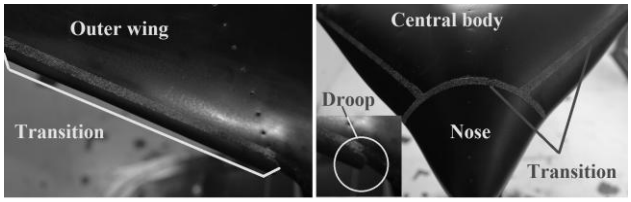

a) Transition at outer wing b) Transition at central body

Fig 6 Transition strips

A balance able to measure two force components is adopted. This device has, at maximum loading, measurement accuracy of +0.7%, therefore, for lift and drag the accuracies are +1.0 N and +0.19 N, respectively.

4 Results and discussion

This paper presents four configurations: with droop, adopted as the baseline geometry with results shown in the following; winglet, C-wings and an arrangement of three fences, see Fig. 6.

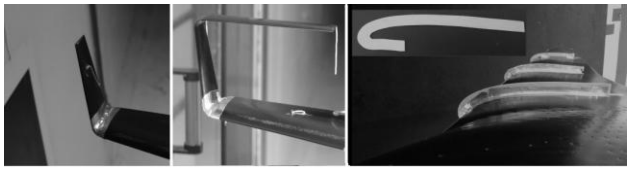

a) Winglet b) C-wing c) Wing-fences

Fig 6 Configurations tested

4.1 Droop effects

Figure 7 shows the lift coefficient curve for first prototype and the new baseline configuration. The droop effect is analyzed in two phases of the lift coefficient curve: firstly for $\alpha<9^o$, where the curve slope is increased by the droop due to the favorable pressure gradient raise; secondly, when $\alpha>9^o$, the slope was decreased. Noteworthy the C_L tends to be the same value at high angles-of-attack.

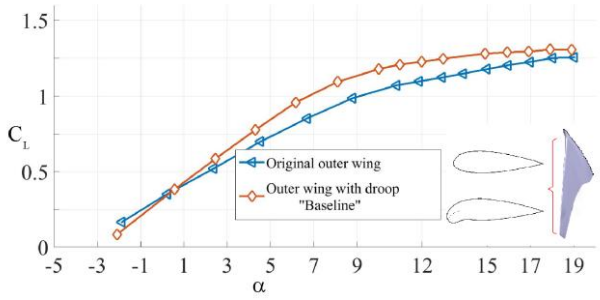

Fig 7 Comparative curves of C_L with droop

The results shows that the central body is the main lift generator $\alpha>9^o$ and the outer wing separation is predominantly related to the swept angle and not to the airfoil camber. Oppositely, the droop modifies the C_D behavior for $\alpha>9^o$, e.g. the drag coefficient is lower for the same lift coefficient (Fig. 8).

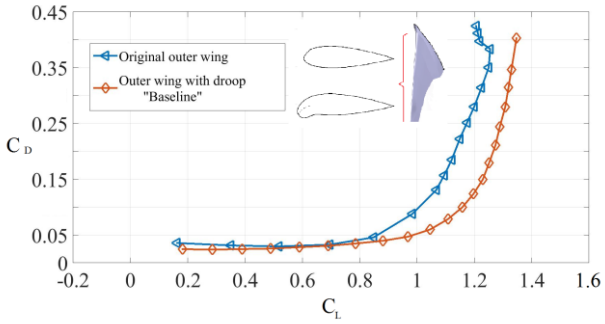

Fig 8 Comparative curves of C_D with droop

4.2 Aerodynamic coefficients for Winglet, C-wing and Fences

The lift coefficient curves shown in Fig. 9 demonstrates that the fences reduce the lift at angles-of-attack between 4^o and 12^o. However, for $\alpha>12^o$ this behavior is changed and the lift is superior, compared with the baseline configuration.

The winglets produce similar C_L values when compared to the baseline configuration for $-4^o\leq\alpha\leq 6^o$, however, between 6^o and 12^o the lift coefficient is thinly reduced. The C-wing configuration presents no differences with baseline until $\alpha\geq8^o$ where the C_L is increased. Unlike the winglet, there is an horizontal surface on the C-wing which can generate a

vertical component force, contributing to enlarge the resultant aerodynamic force.

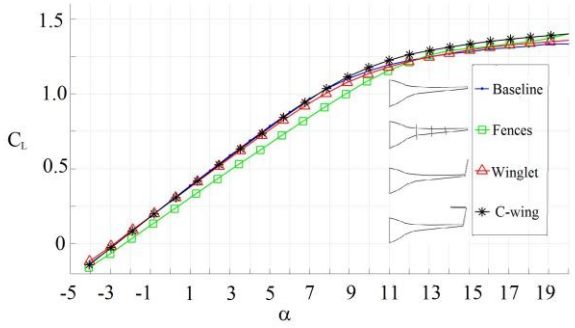

Fig 9 Lift coefficient curves

There are no considerable differences in the drag coefficient among the configurations, except to the fences, where the drag is higher when the C_L is lower than 1.2 approximately. From this point, all configurations contribute to the drag reduction as observed in the Fig. 10.

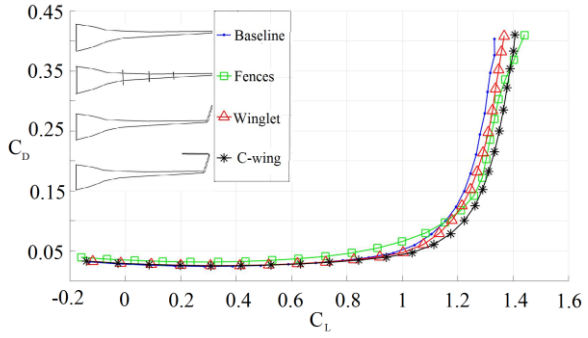

Fig 10 Drag coefficient curves

Figure 11 shows that the fences reduce significantly the aerodynamic efficiency, while the wing tip devices improve it. The C-wing presents the best behavior in this topic, reaching both the highest efficiency value at greater angle of attack, $\alpha=8^o$ whereas the maximum efficiency is attained at $\alpha=5^o$ by the baseline model.

Considering that the wing overall drag coefficient is represented by:

$$C_D = C_{Do} + kC_L^2 \qquad (1)$$

where C_{Do} is the zero-lift drag coefficient and k is the slope of the respective curve. The induced drag effects shown in Fig. 12 demonstrates that as the central body vortex affects strongly the lift generation, the curve is not totally linear. However it is possible observe that the wing tip devices increases the zero-lift coefficient and the derivative of the curve was reduced, specially by the C-wing. Therefore, the winglets and the C-wings were able to considerably reduce the induced drag. Regarding the fences, there is no effect in the induced drag, however the overall drag is increased.

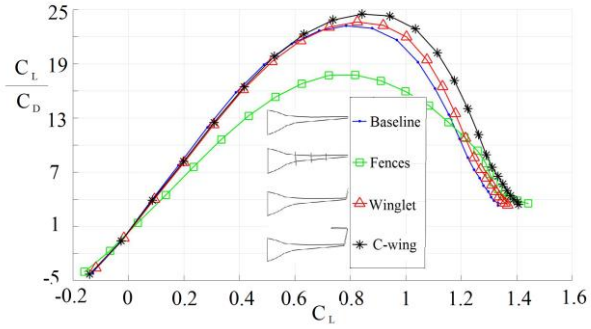

Fig 11 Aerodynamic efficiency curves

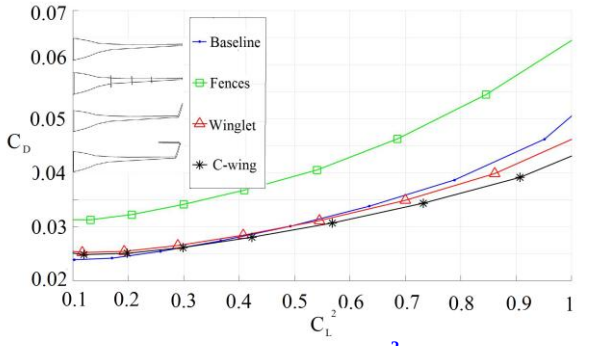

Fig 12 C_D Vs C_L^2

4.3 Oil flow visualization

A mixture of titanium oxide, vegetable oil and paraffin was impregnated on the model with objective of visualize the flow path on the aerodynamic surfaces. Firstly, only the outer wing is tripped therefore it is observed a big bubble in the central body, therefore it is decided to fix the transition in the central body, as previously mentioned. Figure 12 shows that as the bubble is broken the flow path is modified.

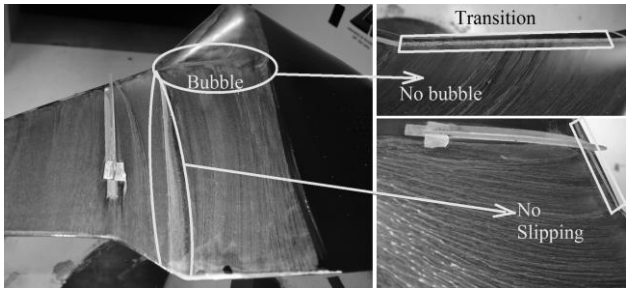

Fig 12 Transition effects on the central body

Due to the low Reynolds number of the C-wing, the horizontal surface was tripped. Figure 13 shows the C-wing with and without transition.

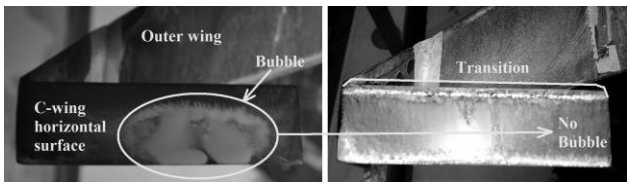

Fig 13 Transition effects on the C-wing

Finally, Fig. 14 shows the presence of a cross flow on the outer wing at $\alpha=8^o$, in despite of the presence of the droop and the fences. Oppositely, at $\alpha=20^o$, the height and length of the internal fence is not satisfactory to avoid the cross flow due to the strength vortex produced in the central body going toward outer wing.

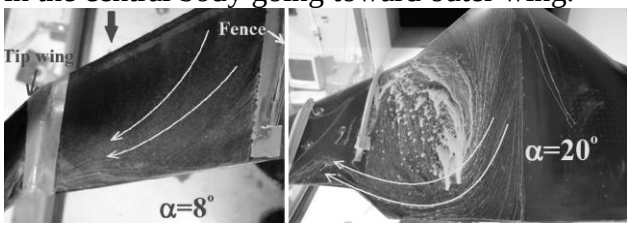

Fig 14 Oil flow visualization

4 Conclusions

This paper shows that the BWB aerodynamics is divided in two main surfaces: the outer wing and the central body. The central body behaves similarly to a delta wing, producing lift through two strong vortices. However, the aerodynamic outer wings are affected by these vortex, therefore presenting a satisfactory behavior at low angles of attack.

A droop is added to the outer wing leading edge to delay the flow separation in this surface. Even though the CL is improved the outer wing stall remains unaltered. The fences showed inefficient to attenuate the cross flow present in this surface at high angles of attack. Additionally the drag is increased and the lift reduced by the presence of the fences.

Besides the fact that the outer wing aerodynamic performance is not totally satisfactory, it is possible to analyze the winglets and C-wing effects. Those devices improved the aerodynamic efficiency as well as reducing the curve slope C_D x C_L^2. Comparing these wing tip devices, the C-wing is the most promising feature.

References

[1] A. L. Bolsunovsky, N. P. Buzoverya, B. Gurevich,V. Denisov, A. Dunaevsky, L. Shkadov, O. Sonin, A. Udzhuhu, and J. Zhurihin, "Fying wing-problems and decisions," *Aircraft Design*, vol. 4, no. 1, pp. 193–219, 2001.

[2] Kuntawala B. N., Hicken E. J. and Zingg W.D. Preliminary Aerodynamic Shape Optimization of a Blended Wing Body Aircraft Configuration. *49TH AIAA Aerospace Sciences Meeting Including the New Horizons Forum and Aerospace Exposition*, Orlando, Florida, 2011.

[3] C. A. Hall and D. Crichton, Engine design studies for a silent aircraft, *Journal of Turbomachanary*, vol. 129, no. 3, pp. 479–487, 2007.

[4] H. H.Ghigliazza, R. Martinez-Val, and E. Perez, Wake of transport flying wings, *Journal of Aircraft*, vol. 44, no. 2, pp. 558–652, 2007.

[5] R. Martínez-Val, E. Pérez, P. Alfaro, and J. Pérz, Conceptual design of a medium size flying wing, *Journal of Aerospace Engineering*, vol. 221, no. G1, pp. 57–66, 2007.

[6] H. D. Ceron-Muñoz and F. M. Catalano, Aerodynamic interference of power-plant system on a Blended Wing Body, *27th International congress of the aeronautical sciences (ICAS)*, 2010

[7] P. M. Bowers, Aeronaves não–conviencionais. Lutécia, 1984.

[8] R. H. Liebeck, M. Page, and B. K. Rawdon, Concepts for advanced subsonic transports, Tech. Rep. CR–4624, NASA Langley Research Center, 1994.

[9] C. L. Nickol, Silent aircraft initiative concept risk assessment, Tech. Rep. TM-2008-215112, NASA Langley Research Center, 2008.

[10] N. Quin, A. Vavalle, L. Moigne, M.Hackett, P. Weinefert, Aerodynamic considerations of blended wing body aircraft. *Progress in Aerospace Sciences*, Vol. 40, No. 6, pp 321-343, 2004.

[11] H. D. Ceron-Muñoz, D. O. Diaz-Izquierdo, J. Solarte-Pineda and F. M. Catalano, Aerodynamic interference of wingtip and wing devices on BEB model, *29th International congress of the aeronautical sciences (ICAS)*, 2014

[12] F. Catalano, The new closed circuit wind tunnel of the aircraft laboratory of university of São Paulo. *16th Brazilian Congress of Mechanical Engineering*, Vol. 6, pp. 306–312.
[13] JR, W. A. N.; SATRAN, D. R. Johnson, joseph l. Jr. Effects of Wing-Leading-Edge Modifications on a Full-Scale, Low-Wing General Aviation Airplane Wind Tunnel Investigation of High-Angle-of-Attack Aerodynamic Characteristics. NASA TP-2011, 1982.
[14] Whitcomb, R. T. A design approach and selected wind tunnel results at high subsonic speeds for wing-tip mounted winglets. *NASA Technical note D-8260*, p. 30, 1976.

8 Contact Author Email Address

mailto: hernan@sc.usp.br

Copyright Statement